

Comparison of empirical models with intensively observed data for prediction salt intrusion in the Sumjin River Estuary, Korea

5 **Dinesh Chandra Shaha ^a, Yang-Ki Cho ^{a,*}**

^a Faculty of Earth Systems & Environment Sciences

Chonnam National University,

10 **Gwangju 500-757, Korea**

* Corresponding author.

E-mail address: ykcho@chonnam.ac.kr (Y.-K. Cho)

15

alison #1
Gay #2

20

Abstract

Intensive measurements of salt intrusion in the Sumjin River Estuary were taken at high
5 and low waters during both spring and neap tides in each season from August 2004 to
April 2007. The estuary demonstrated partially- and well-mixed characteristics during
the spring tide and stratified condition during the neap tide. The salt intrusion at high
water varied from about 13.39 km in summer 2005 to 25.62 km in autumn 2006. The
salt intrusion depended primarily on the freshwater discharges rather than those of
10 spring-neap tidal oscillations. Analysis of three years of observed salinity data indicated
that the salt intrusion length scale in the Sumjin River Estuary was proportional to the
river discharge to the $-1/5$ power. Five empirical models were applied to the Sumjin
River Estuary to explore the most suitable as an easy-to-use tool for prediction of the
salt intrusion length as functions of the geometry, river discharge and tide. Comparative
15 results showed that the Nguyen and Savenije (2006) model developed under both
partially- and well-mixed estuaries yielded the most satisfactory results of all the models
studied for computing the salt intrusion length in the Sumjin River Estuary. Our study
suggests that the model can generate reasonable results for stratified conditions also.

20

Key words: Sumjin River Estuary; salinity intrusion; empirical models; tide

25

1 Introduction

An estuary, which is the transitional area where fresh water meets ~~with~~ saltwater, is known to be one of the most valuable natural, economic and cultural resources. The salinity intrusion in an estuary is maintained by the competition between two opposing longitudinal salt fluxes — an advective flux resulting from freshwater out flow, tending to drive salt out of the estuary; and a ~~down~~ gradient salt flux (fluxes from high to low salinity), tending to drive salt landward (Fischer et al., 1979; Geyer and Signell, 1992). The river discharge, ~~tides~~ and geometry are the key determinants for saltwater intrusion. Water is withdrawn from many rivers for irrigation and drinking purposes. However, water contaminated by salt from the sea is no longer useable (Aerts et al., 2000). Consequently, conflict ~~s~~ may arise between those withdrawing water upstream ~~of the river~~ and those who are affected by the high ~~salinity~~ salt wedge downstream ~~of the estuary~~.

The Sumjin River estuary is one of the few natural estuaries located on the south coast of Korea. ~~An~~ ^{ing} increased upstream seawater intrusion is the major environmental issue of this estuary, which ~~might~~ ^{may} be caused by withdrawing excessive ^(affecting base flow) groundwater, an upstream dam construction ~~that~~ ^{ins} decreases ~~the~~ stream flow, ^{and} extraction of sand and gravel, which lowers the stream bottom level (Lee, 2005). Therefore, an instrument is essential to assess the salt intrusion length as a function of directly measurable parameters, such as geometry, freshwater discharge and tide, to mitigate this problem. There are three main study methods for detecting saltwater intrusion; the material analysis method, the empirical correlation method and the use of numerical simulation technology. Based on the material analysis method, Pritchard (1956) and Bowden (1966) explain the distribution of saltwater and the mixing characteristics of saltwater

and freshwater. The empirical correlation method refers to searching for empirical formula with a large number of historical data relating to the river discharge and salinity in estuaries and forecasting the effect on saltwater intrusion by changes in a river's discharge. Based on the balanced equation of salinity combined with hydrodynamic equations, numerical simulation technology can determine the different influences on saltwater intrusion under different boundary conditions.

5

here also predictive equations for salt intrusion are required. Thinking that he would do it is a mistake.

As the numerical modeling for seawater intrusion in an estuary is time-consuming and expensive, it is preferable to use tools such as empirical models for the rapid assessment

wrong reason

10

of salt intrusion. Two types of predictive models currently exist - those based on laboratory experiments in channels of constant cross-section and those based on a real environment. Van der Burgh (1972), Rigter (1973), Fischer (1974), Van Os and

estuaries

Abraham (1990) and Savenije (1993) performed empirical works for predicting salinity intrusion. Except for the models of Van der Burgh (1972) and Savenije (1993), who

15

carried out their works considering real environments, all the models are based on laboratory experiments and prototype measurements in estuaries. Savenije (1993) use an

exponential function to describe the estuarine geometry for predicting the salt intrusion length, whereas Thatcher and Harleman (1972) reported the geometrical character of

used the observed cross-sections?

20

the estuary. In 2005 Savenije slightly generalized and improved his 1993 model based on well-mixed alluvial estuaries. Nguyen and Savenije (2006) further elaborated this method to include partially- and well-mixed estuaries.

an enlarged database of

elaborated

to include

The main purposes of this study ^{is} were to: (i) compare the performance of different existing empirical models with three years observation data obtained at high water ^{slack?} during both spring and neap tides for each season from August 2004 to April 2007, (ii) determine the most suitable model for predicting salt intrusion in the Sumjin River Estuary, and (iii) examine whether the model developed by Nguyen and Savenije (2006) for partially- and well-mixed estuaries ^{is} was applicable to the stratified Sumjin River Estuary.

2 Data sources

10 The Sumjin River estuary falls into the Gwangyang Bay located in the south coast of Korea (Fig. 1). The length of the main stream is ~~about~~ 212.3 km, with a watershed area of almost ⁴⁹⁰⁰ 4,897 km², including farmland. A tributary, namely Hwangchon, exists at around 12 km from the river mouth. The deepest point at high water is no more than 17 m down ^{stream} stream of the estuary, with the upper estuary being only a few meters deep. The topographic information surveyed in 1994 ^{has been} was collected from the Regional Construction and Management Office of the Construction Department, the Ministry of Construction. The cross-sectional area (m²), width (m) and mean depth (m) of this river ^{from} the mouth ^{seaward} (station 1) to a landward location (station 25) are shown in Fig. 2. The convergence lengths of the cross-sectional area (a) and width (b) are 12,600 and 87,229 ²⁰⁰ m, respectively •

Why not make logarithmic plots, showing the conv. length.
Why not more width values?

Freshwater inflows to rivers are usually measured by gauges located either in the tributaries or upstream of the river. The river discharge data of the Songjung gauge station located about 10 km upstream from CTD station 25 were used in this study. The

river discharge and tidal range on the day of field observation from July 2004 to June 2007 are given in Table 1. The climate of Korea is characterized by four distinct seasons: spring, summer, autumn and winter. The summer season, in general, is more prone to high river discharges, while the remaining seasons are susceptible to low river discharges. The tidal information was collected from the Gwangyang Tidal Station (see in Fig. 1) operated by the National Oceanographic Research Institute, Korea. The tidal cycle is semi-diurnal, with mean spring and neap ranges of 3.33 and 1.02 m, respectively, based on the field observations. Based on the tidal range of Davies (1964), this estuary can be characterized as mesotidal during spring tide and microtidal during neap tide. The M_2 tide (1.06 m) is the primary tidal constituent at the river mouth.

The longitudinal transects for salinity and temperature were taken at high and low waters during both spring and neap tides for each season from August 2004 to April 2007 using a CTD profiler (IDRONAUT Company). GPS was used to obtain the exact locations. The nominal distance between CTD stations was 1 km. The measurement starts from the river mouth one hour before high or low waters and takes about one hour to cover all the stations (Fig. 1). The number of observation stations along the estuary for each cruise varied between 13 and 25 depending on the change in the water depth with the tide.

20

3 Empirical Models Description

Empirical models were applied to the Sumjin River Estuary as easy-to-use tools for predicting the salt intrusion length as a function of the geometry, freshwater discharge and tide. The most important output of these models is the salt intrusion length. In this study, the salt intrusion length at high water during both spring and neap tides was defined as the length from the river mouth (station 1) along the river channel to the point where the salinity at the bottom was 1. The empirical models used are listed in the Table 2. L^{LWS} is the intrusion length at low water slack (LWS); the minimum intrusion length occurring during a tidal period. L^{HWS} is the intrusion length at high water slack (HWS); the maximum intrusion length during a tidal period and L^{TA} is the tidal averaged intrusion length. h_0 is the tidal average depth, f Darcy-Weisbach's roughness, F_d the densimetric Froude number, F the Froude number, N the Canter-Cramers estuary number, a the area convergence length, Q_f the river discharge, D_0 the dispersion coefficient ^{near the mouth} and K Van der Burgh's coefficient (Table 2). Savenije (2005) elaborately presents a predictive model for the salt intrusion in well-mixed alluvial estuaries. The area convergence length (a) and the width convergence length (b) are defined as:

$$A = A_0 \exp\left(-\frac{x}{a}\right) \quad (6)$$

$$B = B_0 \exp\left(-\frac{x}{b}\right) \quad (7)$$

where A_0 and B_0 are the tidal average cross-sectional area and width at the estuary mouth ($x = 0$), respectively. The model developed by Savenije (1993) has been applied to 17 different estuaries all over the world, particularly for the HWS situations, with two predictive equations derived for K and D_0^{HWS} . These relations were initially generalized

and improved by Savenije (2005) and later by Nguyen and Savenije (2006) for partially- and well-mixed estuaries, as given below:

$$D_0^{HWS} = 1400 \frac{\bar{h}}{b} \sqrt{N_R} (\nu_0 E_0) \quad (8)$$

$$K = 0.2 \times 10^{-3} \left(\frac{E}{H} \right)^{0.65} \left(\frac{E}{C^2} \right)^{0.39} (1 - \delta)^{-2.0} \left(\frac{b}{a} \right)^{0.58} \left(\frac{Ea}{A_0} \right)^{0.14} \quad (9)$$

5 where \bar{h} is the average depth over the salt intrusion length. E_0 is the tidal excursion at the estuary mouth, the difference between the intrusion length at HWS and LWS. ν_0 is the tidal velocity amplitude at the estuary mouth, H the tidal range, C the Chezy coefficient, δ the damping rate of the tidal range and N_R the estuarine Richardson number. The damping rate of the tidal range and N_R are defined as:

$$10 \quad N_R = \frac{\Delta\rho}{\rho} \frac{g\bar{h}Q_f T}{A_0 E_0 \nu_0^2} \quad (10)$$

$$\delta_H = \frac{1}{H} \frac{\partial H}{\partial x} \quad (11)$$

Van der Burgh (1972) provides a formula using limited field observations in real estuaries, for example the Rotterdam Waterway, the Schelde and the Haringvliet. Rigter (1973) provided an empirical relation based on the flume data of the Delft Hydrodynamics Laboratory and the Waterways Experiment Station (WES). Moreover, Fischer (1974) gave a formula based on the same data. Van Os and Abraham (1990) developed a formula like that of Rigter (1973) for Delft Hydraulics. Except the models of Van der Burgh (1972) and Savenije (2005), all the models are based on laboratory ~~tests and prototype measurements in estuaries~~ ^{experiments}. Savenije (1993) used the exponential function for estuarine geometry for predicting the salt intrusion length and Eqs. (6) and (7) as exponential functions for longitudinal variations of the cross-sectional area and

width of estuaries. In 2005, Savenije generalized and improved his 1993 model based on well-mixed alluvial estuaries, with further modifications by Nguyen and Savenije (2006) based on partially- and well-mixed estuaries.

5

4 Results

4.1 Measurement of saltwater intrusion

The longitudinal sections of salinity and temperature were observed at high and low waters during both spring and neap tides for each season from August 2004 to April 10 2007. Each cruise was started from the mouth about one hour before high water and took approximately one hour to arrive at the last station. As all landward stations were unable to be surveyed at low water, data taken during these periods were discarded as they did not fulfill the measurement criteria of salinity 1. In this study, the salt intrusion length at high water during both spring and neap tides was defined as the length from 15 the river mouth (station 1) along the river channel to the toe point where the salinity was 1. Moreover, the field data were extrapolated in the absence of salinity 1. ?

? not at tides

?

1 ‰

The estuary exhibited a complex vertical salinity distribution during spring tide due to the abruptly varying bottom topography, and variable river discharge and tidal 20 oscillations. The entire water column of the estuary ~~was~~ oscillated by tide during the spring tide. In contrast, the salinity distribution pattern during ~~the~~ neap tide was comparatively simpler than ~~that~~ during ~~the~~ spring tide. Based on the salinity structure (Dyer, 1997) and stratification parameter (Hansen and Rattray, 1966), the Sumjin River

?
I would expect the reverse

Estuary ^{is} was found to be a partially- and well-mixed estuary during the spring tide and a stratified estuary during the neap tide.

? The horizontal bottom salinity distributions taken at high water during spring tide in 2005 and during neap tide in 2006 ^{are} were plotted, as ~~shown~~ in Figs. 3 and 4. How the variable river discharges and tide affect the salt intrusion during both spring and neap tides was then assessed. A high river discharge appeared during summer, with tidal amplitude of 1.0 - 1.5 m, ^{and} ~~and~~ the other seasons were usually susceptible to lower river discharges, with tidal amplitude of 1.5 - 2.0 m during the study period. The maximum intrusion length, about ²⁶ ~~25.62~~ km, occurred for a low river discharge during the spring tide on 6 November 2006, while the minimum, around ¹³ ~~13.39~~ km, occurred at a high river discharge during the neap tide on 21 July 2005.

Why not graphs

The salt intrusion length increased ^{with} by about 4 and 3 km during the spring tide of spring and autumn 2006 compared to ^{or} for the same period in 2005. This ^{is due} ~~seemed~~ to be related to the river discharge and tide. In spring, the intrusion length ^{was} might increase due to the 9% greater tidal amplitude and 39% lower river discharge. Similarly, in autumn, the river discharge was about 50% less than the previous year, whereas the tidal amplitude remained approximately the same. This indicated ^s that the autumn length was solely affected by the freshwater flow. ^{During Summer} However, the intrusion length was approximately the same ^{at} during the spring tide ~~in summer~~. The intrusion length was a little bit high during the neap tide for both summer and autumn 2006 compared to the same period in 2005.

The freshwater discharge was 42% less, whereas the tidal range was 19% less during summer 2006. ^{Therefore} Both the freshwater discharge and tide ^{the} might; ^{are likely} ~~therefore~~, be the potential causes for the summer increase of salt intrusion. Conversely, the tidal range during the

neap tide in autumn 2006 became doubled, but the freshwater discharge was almost the same (Table 1). This indicated^s that the tidal amplitude ~~might be~~ⁱ the reason for the autumn increase in the salt intrusion during 2006. The tidal excursions, the distance between the low and high water locations of a vertically-mixed parcel of water, ~~were~~^{was} measured during ~~the~~ spring tide in relation to the location of salinity 27. Tidal excursions ranged between 3 and 9 km during ~~the~~ spring tide (Table 3).

→ how were these measured? , if no observation at LWS? ? station? %/oo ?

4.2 Model intrusion length

10 The ^{most} important output of the empirical models is the salt intrusion length. However, the salt intrusion primarily depends on variable river discharges, the geometry of the estuary and the tide. Van der Burgh's coefficient, K , was calculated from the field data using Eq. (10). The value of this coefficient was 0.76; within the range 0 to 1. The Darcy-Weisbach friction factor ($f_D = 8g/C^2$) was 0.024. As the observed intrusion length ^{determined} was ~~found~~ under a high water slack situation and the models of Rigter (1973), Fischer (1974), Van Os and Abraham (1990) are based on low water slack, the tidal excursion, E , was added to obtain the high water slack intrusion length; however, half the tidal excursion ($E/2$) was added in the case of Van der Burgh (1972) as this is a tidal average model.

20

Comparisons between the model results and field data are shown in Fig. 5. The Fischer (1974) model provided poor results. Furthermore, no significant variation in the model results between Rigter (1973) and Van Os and Abraham (1990) was found since the formulas used for both models are quite similar, but varied greatly with the observed

lengths. Darcy-Weisbach's coefficient, solely a function of flow roughness, is accounted for in the above three models. Moreover, the Savenije model (2005) overestimated the salt intrusion length as it uses the area convergence length (a) for calculating the dispersion coefficient (Fig. 5). Conversely, the best result was obtained from the modified model given by Nguyen and Savenije (2006) compared to those using Van der Burgh (1972) and Savenije (2005). The Van der Burgh coefficient, K , is used in these two models, which is ^{a} functions ^{$average$} of both ^{a} tidal and freshwater flow characteristics.

10 In our study, the daily mean freshwater discharge was used. Considering all of the tidal parameters at the estuary mouth, freshwater discharges and the geometry of the estuary, the Nguyen and Savenije (2006) model yielded the most significant results for the Sumjin River Estuary of all the models studied (Fig. 5). This model was found to be highly capable for computing the salt intrusion length for two reasons. Firstly, it contains an exponential function for the estuarine geometry. Secondly, it contains more parameters than the other existing models. Parsa et al. (2007) obtained satisfactory result from the Van der Burgh model (1972) compared to Savenije (1993) using the annual average discharge. Parsa et al. (2007) quoted that the salinity intrusion strongly depended on the river flow as well as the morphological characteristics, but they considered only one river discharge; the annual average for a single intrusion length. However, Skreslet (1986) reported that variability in freshwater flow was the predominant source of seasonal variation in estuaries, and freshwater influences the physics, geology, chemistry and biology of estuaries in a variety of ways.

4.3 Dominating factor for controlling salt intrusion length

Salt intrusion in estuaries is controlled by various mechanisms, including tidal dispersion, the geometry, vertical mixing and the river flow. Therefore, it is important to

5 examine which external force, either freshwater buoyancy input or tide, is the predominant function for salt intrusion in an estuarine system. Under steady state or

tidally averaged (spring-neap tidal cycle) conditions, the salt intrusion length scale, X_s , as a function of river flow can be described by the power-law relation (Hansen and Rattray, 1965; Monismith et al., 2002):

in first order approach may be as a function of the river discharge in prismatic estuaries

10 $X_s \approx Q^\alpha$ (12)

where α is the power dependence coefficient. Previous research has shown that the power dependence coefficient varies widely under different estuarine conditions. The salt intrusion length scale for the Sumjin River Estuary is proportional to the river discharge to the -1/5 power based on our three years of observed salinity data (Fig. 6).

15 Monismith et al. (2002) obtained $\alpha \sim -1/7$ for their 21 years of observed salinity data for San Francisco Bay. Furthermore, another linear least square regression was developed

between high water levels and measured distance to prove that either the tide or river discharge or both are the dominant factor in controlling the salt intrusion in this estuarine system. The regression fitting indicated that the salt intrusion upstream of the estuary primarily depended on the river discharges, but to a lesser extent on the spring-neap tidal oscillations. Uncles and Stephens (1996) found that the salt intrusion was a strong function of the spring-neap tidal state, but a weaker function of the freshwater inflow in the Tweed Estuary, UK.

Which? Where?

20

Where? by whom?

It has been demonstrated before (e.g. Saviniev, 2005) that because of the assumption used of a constant cross-sectional area, different estuaries have different exponents

Who says that?
In general,

5 Discussion

Tide-driven mixing was dominant downstream, but gravitational mixing upstream of the estuary. Van der Burgh coefficient, K , gives a solution for both mechanisms (Savenije, 2006).

5 2006). Tide-driven mixing becomes dominant near the toe of a salt intrusion when K is small. By contrast, if K approaches unity, then gravitational mixing becomes dominant. In our study, the value of K for the Sumjin River Estuary was 0.76, indicating that the gravitational flux was important near the toe of the salt intrusion. In addition, the flushing rate can be used as an index parameter for both tidal and gravitational mixing (Officer and Kester, 1991). The flushing rate (F) is the rate at which the freshwater exchanges with the sea. The flushing rate is defined as follows:

$$F = \frac{V}{\tau} = \frac{s_{sw}}{s_{sw} - s} R \quad (13)$$

where V is the volume of the estuary portion being considered, τ the flushing time, s the volume-averaged salinity of the estuary portion being considered, s_{sw} the salinity of sea water and R the river discharge. The flushing time (τ) is calculated using the following formula:

$$\tau = \frac{V_f}{R} \quad (14)$$

where V_f is the freshwater volume of the estuary portion being considered. V_f can be defined as follows:

$$20 \quad V_f = \left(1 - \frac{s}{s_{sw}}\right) V \quad (15)$$

The quantity, F , which has the dimension of $\text{m}^3 \text{s}^{-1}$, represents the combined effects of the tidal exchange and the gravitational exchange flux. The tidal exchange flux should be independent of the river discharge, but the gravitational circulation flux strongly

depends on the river discharge. If there are no tidal exchanges, a plot of F against R will give a line with an intercept ^{of} at zero. If both the tidal exchange and gravitational circulation flux are ^{active} operative, there should ^{be} have an intercept value, F_{int} that represents the tidal exchange flux and the excess amounts of the intercept ~~value~~ represent the gravitational circulation flux. This method was first applied to the Narragansett Bay by Officer and Kester (1991). To determine the fluxes the freshwater inputs, the corresponding values of the average salinity of the estuary portion being considered and the salinity of the adjacent sea are required. This technique ^{has been} was applied to the upper Sumjin River Estuary, ^{near the toe of the salinity curve} ~~the fluctuated zone of intruded salinity~~ ^{ppt 10} depending on the tide and freshwater discharge, by dividing it into two segments. Segment A contains the stations 21, 22, 23, 24, 25 and segment B the stations 17, 18, 19 and 20. Analysis of three years of observed salinity data indicated ^s that the gravitational flux ^{is} became dominated ⁱⁿ on the segment A whereas ⁱⁿ the segment B ^{is a} was a combination of the gravitational circulation flux and tidal flux. But the small intercept ~~value~~, F_{int} for ~~the~~ segment B implies ~~the~~ strong gravitational circulation flux ^a and weak tidal flux. Therefore, the zone of ~~intruded salinity~~ ^{of the salt intrusion curve} near the toe ~~upstream~~ ^{for a t} for the maximum salt intrusion length ⁱ was dependent on the gravitational flux (Fig. 7). The Van der Burgh coefficient; thus, corresponded ^s well with the gravitational flux. Although the Van der Burgh coefficient is slightly more complex to solve than that of the simplified method given by Officer and Kester (1991), it is also a good indicator for determining the gravitational flux near the toe of a salt intrusion. Indicator

Equation (8) was slightly modified by Nguyen and Savenije (2006) by replacing the area convergence length with the width convergence length and the average depth over

the salt intrusion length for partially- and well-mixed estuaries. The Sumjin River Estuary shows well- and partially-mixed characteristics during ~~the~~ spring tide, but stratified conditions during ~~the~~ neap tide. The slightly modified equation for the dispersion coefficient works better during ~~the~~ spring than ~~the~~ neap tide (Fig. 8). The method is also applicable to the stratified Sumjin River Estuary for predicting the salt intrusion length. It should be noted that the use of the width convergence length rather than the area convergence length when calculating the dispersion coefficient results in a more reasonable prediction of the salt intrusion length.

The width convergence length is simpler and less demanding. (data)

10 6 Summary

Intensive field measurements were carried out for three years to observe the salt intrusion at high and low waters ~~during~~ both spring and neap tides in the Sumjin River Estuary. The estuary demonstrated partially- and well-mixed characteristics during ~~the~~ spring tide, but stratified conditions during ~~the~~ neap tide. From our field observations, the salt intrusion at high water varied from about 13.3⁴~~9~~ km in summer 2005 to 25.6~~2~~ km in autumn 2006. The salt intrusion upstream primarily depends on river discharges rather than on spring-neap tidal oscillations. Analyses of the three years of observed salinity data indicated that the salt intrusion length scale in the Sumjin River Estuary ~~was~~ ^{is} proportional to the river discharge to the $-1/5$ power. The Van der Burgh coefficient ~~was~~ ^{is} a good indicator for determining the gravitational flux near the toe of the salt intrusion.

have been
Five empirical models ~~were~~ applied to the Sumjin River Estuary for predicting the salt intrusion. Comparative results showed ~~ed~~ that the Nguyen and Savenije (2006) model,

developed under partially- and well-mixed estuaries, yielded^s the most satisfactory result of all the models studied for predicting the salt intrusion in the Sumjin River Estuary. ^{The fact that} As the model used^s an exponential function of varying cross-section areas, ~~as well as~~^{and} containing^s more parameters than the other existing models, ~~might be the~~^{in the} probable cause ^{its} for the high capability ^{to} in computing^e the salt intrusion length. Our study suggests that the model is also applicable to the stratified Sumjin River Estuary. Hydrodynamic processes in estuaries and coastal seas are generally 3-D tidal flows in a setting of complex geometry and bottom topography. Therefore, a 3-D hydrodynamic model is in the development stage to gain a better understanding of the salinity distribution and circulation pattern of estuarine systems, including the Gwangyang Bay.

Acknowledgements

The authors would like to acknowledge the members of the Earth Environment Prediction Laboratory for their enthusiastic supports during the data collection period.

References

Aerts, J. C. J. H., Hassan, A., Savenije, H. H. G. and Khan, M. F.: Using GIS tools and rapid assessment techniques for determining salt intrusion: STREAM, a river basin management instrument, *Physics and Chemistry of the Earth*, 25, 265-273, 2000.

Bowden, K. F.: The circulation, salinity and river discharge in the Mersey Estuary, *Geophys. J. Roy. Astron. Soc.*, 10, 383-400, 1966.

Davies, J. H.: A morphogenetic approach to world shorelines, *Zeitschrift für Geomorphologie*, 8, 127-142, 1964.

- Dyer, K. R.: "Estuaries, A Physical Introduction", second ed. John Wiley, London, 195pp, 1997.
- Fischer, H. B., List, E. J., Koh, R. C. Y., Imberger, J. and Brooks, N. H.: Mixing in Inland and Coastal Waters, Academic Press, 483 pp, 1979.
- 5 Fischer, H. B.: Discussion of 'Minimum length of salt intrusion in estuaries' by B. P. Rigter, 1973, Journal of Hydraulic Division Proceedings, ASCE, 100, 708-712, 1974.
- Geyer, W. R. and Signell, R. P.: A reassessment of the role of tidal dispersion in estuaries and bays, *Estuaries*, 15, 97-108, 1992.
- 10 Hansen, D. V., Rattray, M. Jr.: Gravitational circulation in straits and estuaries, *J. Mar. Res.*, 23, 104-122, 1965.
- Hansen, D.V., Rattray, M. Jr.: New dimensions in estuary classification, *Limnol. Oceanogr.*, 11, 319-326, 1966.
- Lee, C. H.: Development of sustainable estuary management strategy in Korea II, Korea environment institute, Seoul, 2005.
- 15 Monismith, S. G., Kimmerer, W., Burau, J. R., Stacey, M. T.: Structure and flow-induced variability of the subtidal salinity field in northern San Francisco Bay, *J. Phys. Oceanogr.*, 32, 3003-3019, 2002.
- Nguyen, A. D. and Savenije, H. H. G.: Salt intrusion in multi-channel estuaries: a case study in the Mekong Delta, Vietnam, *Hydrol. Earth Syst. Sci.*, 10, 743-754, 2006.
- 20 Officer, C. B. and Kester, D.R.: On estimating the non-advective tidal exchanges and advective gravitational circulation exchanges in an estuary, *Estuar. Coast. Shelf S.*, 32, 99-103, 1991.
- 25 Parsa, J., Etemad-Shahidi, A., Hosseiny, S. and Yeganeh-Bakhtiary, A.: Evaluation of computer and empirical models for prediction salinity intrusion in the Bahmanshir Estuary, *J. Coastal Res.*, 50, 658-662, 2007.

- Pritchard, D. W.: The dynamic structure of a coastal plain estuary, *J. Mar. Res.*, 15, 33-42, 1956.
- Rigter, B. P.: Minimum length of salt intrusion in estuaries, *Journal of Hydraulic Division Proceedings, ASCE*, 99, 1475-1496, 1973.
- 5 Savenije, H. H.G.: Predictive model for salt intrusion in Estuaries, *J. Hydrol.*, 148, 203-218, 1993.
- Savenije, H. H. G.: *Salinity and Tides in Alluvial Estuaries*, Elsevier, Amsterdam, 197pp, 2005.
- Savenije, H. H. G.: Comment on “A note on salt intrusion in funnel-shaped estuaries: Application to the Incomati estuary, Mozambique” by Brockway et al. (2006),
10 *Estuar. Coast. Shelf S.*, 68, 703-706, 2006.
- Skreslet, S.: *The Role of Freshwater Outflow in Coastal Marine Ecosystem*, NATO ASI Series, Springer-Verlag, Berlin, Germany, 1986.
- Thatcher, M. L. and Harleman, D. R. F.: A mathematical model for the prediction of
15 unsteady salinity intrusion in estuaries. R. M. Parsons Laboratory for Water Resources and Hydrodynamics, Report No. 144, Department of Civil Engineering, MI, 1972.
- Uncles, R. J. and Stephens, J. A.: Salt intrusion in the Tweed estuary, *Estuar. Coast. Shelf S.*, 43, 271-293, 1996.
- 20 Van der Burgh, P.: Ontwikkeling van een methode voor het voorspellen van zoutverdelingen in estuaria, kanalen en zeeën, *Rijkswaterstaat Rapport (in Dutch)*, 10-72, 1972.
- Van Os, A. G. and Abraham, G.: Density currents and salt intrusion, Lecture note for the hydraulic engineering course at IHE-Delft hydraulics, The Netherlands, 1990.

25

30

Table 1. River discharges and tidal ranges during the three year field observations

Years	Seasons	Tidal states			
		Spring		Neap	
		River discharges (m ³ s ⁻¹)	Tidal ranges (m)	River discharges (m ³ s ⁻¹)	Tidal ranges (m)
2004	Summer	46	3.09	22	1.22
2004	Autumn	29	3.86	26	1.60
2005	Winter	10	3.14	16	1.04
2005	Spring	18	3.51	26	0.73
2005	Summer	58	2.45	77	1.20
2005	Autumn	16	3.92	13	0.97
2006	Winter	19	3.17	14	1.12
2006	Spring	11	3.84	30	0.52
2006	Summer	50	2.93	44	0.92
2006	Autumn	9	3.99	15	1.87
2007	Winter	12	3.85	11	1.32
2007	Spring	21	3.03	14	0.84

5

Table 2. Empirical models used for predicting the salt intrusion length

Van der Burgh (1972)	$L^{TA} = 24\pi \frac{h_0}{K} F^{-0.5} N^{-0.5}$	(1)
Rigter (1973)	$L^{LWS} = 4.7 \frac{h_0}{f} F_d^{-1} N^{-1}$	(2)
Fischer (1974)	$L^{LWS} = 17.7 \frac{h_0}{f^{0.625}} F_d^{-0.75} N^{-0.25}$	(3)
Van Os and Abraham (1990)	$L^{LWS} = 4.4 \frac{h_0}{f} F_d^{-1} N^{-1}$	(4)
Savenije (2005)	$L^{HWS} = a \ln \left(-\frac{D_0 A_0}{KaQ_f} + 1 \right)$	(5)

10

Table 3. Estimated tidal excursions during field campaigns

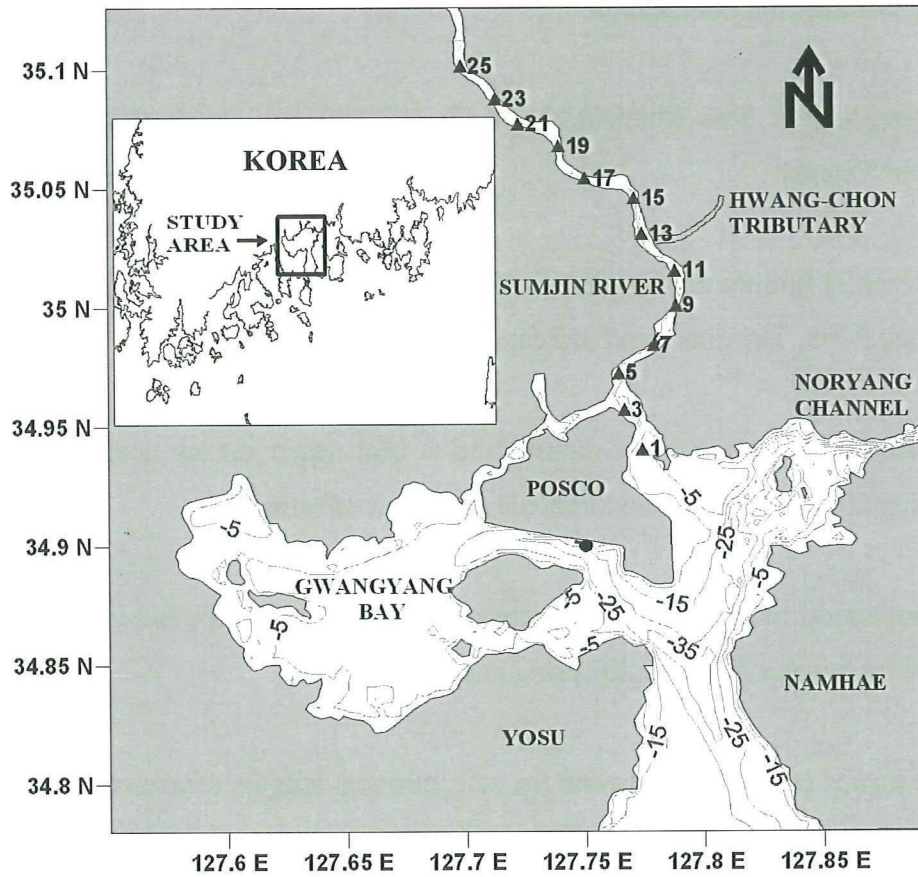
Date	Tidal ranges (m)	Tidal excursions (km)
29/1/2005	2.85	3.36
8/4/2005	3.87	9.37
21/7/2005	2.98	3.00
19/10/2005	3.59	6.76
16/1/2006	2.83	3.09
30/3/2006	3.56	6.96
6/11/2006	3.60	7.97

how did you observe this when you only have HW observations?

List of Figures

- 5 Fig. 1. Map of the study area. The solid triangles indicate CTD stations. The solid circle denotes the Gwangyang tidal station.
- Fig. 2. Cross-section area (diamonds), width (circles) and depth (triangles) of the Sumjin River Estuary.
- 10 Fig. 3. Horizontal bottom salinity distribution at high water during spring tide for each season during 2005. The pink band indicates the limit of salinity 1.
- Fig. 4. Horizontal bottom salinity distribution at high water during neap tide for each season during 2006. The pink band indicates the limit of salinity 1.
- 15 Fig. 5. Comparison of the results of various empirical models for the intrusion length measured at high water during both spring and neap tides.
- 20 Fig. 6. The power correlation between the salt intrusion lengths measured at high water during spring-neap tides and river discharges (upper); observed salt intrusion lengths and high water levels (lower).
- Fig. 7. Plot of flushing rate (F) against river discharge (R) upstream of the Sumjin River Estuary. The upper estuary, segment A, shows gravitational circulation flux where the fitting line is linear with an intercept of zero and increasing F value with increasing R value. The intercept value, F_{int} in Segment B indicates the tidal flux and the excess amount of intercept value indicates the gravitational circulation flux.
- 25 Fig. 8. Comparison of the model results with the intrusion length measured at high water during both spring and neap tides.
- 30

5



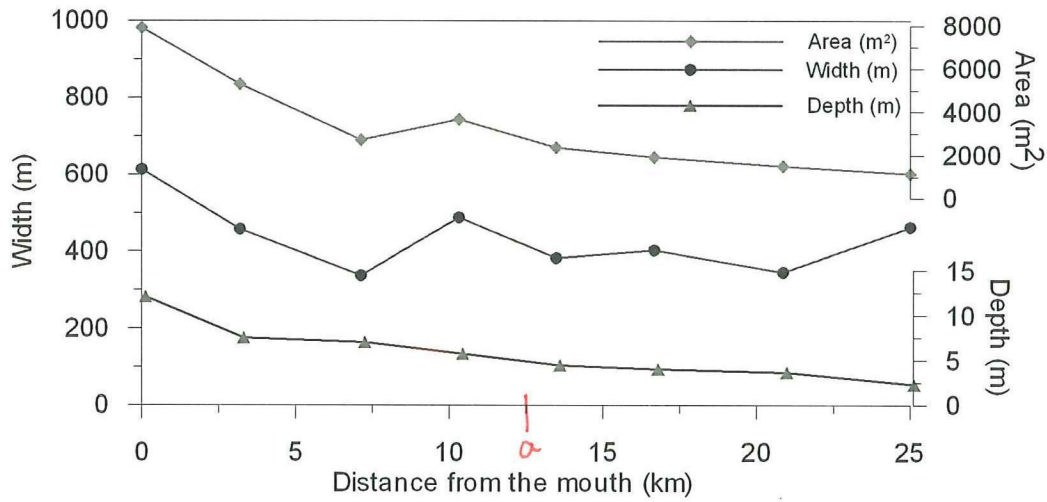
10 Fig. 1. Map of the study area. The solid red triangles indicate CTD stations.
The solid blue circle denotes the Gwangyang tidal station.

15

20

25

5



10 Fig. 2. Cross-section area (diamonds), width (circles) and depth (triangles) of the Sumjin River Estuary.

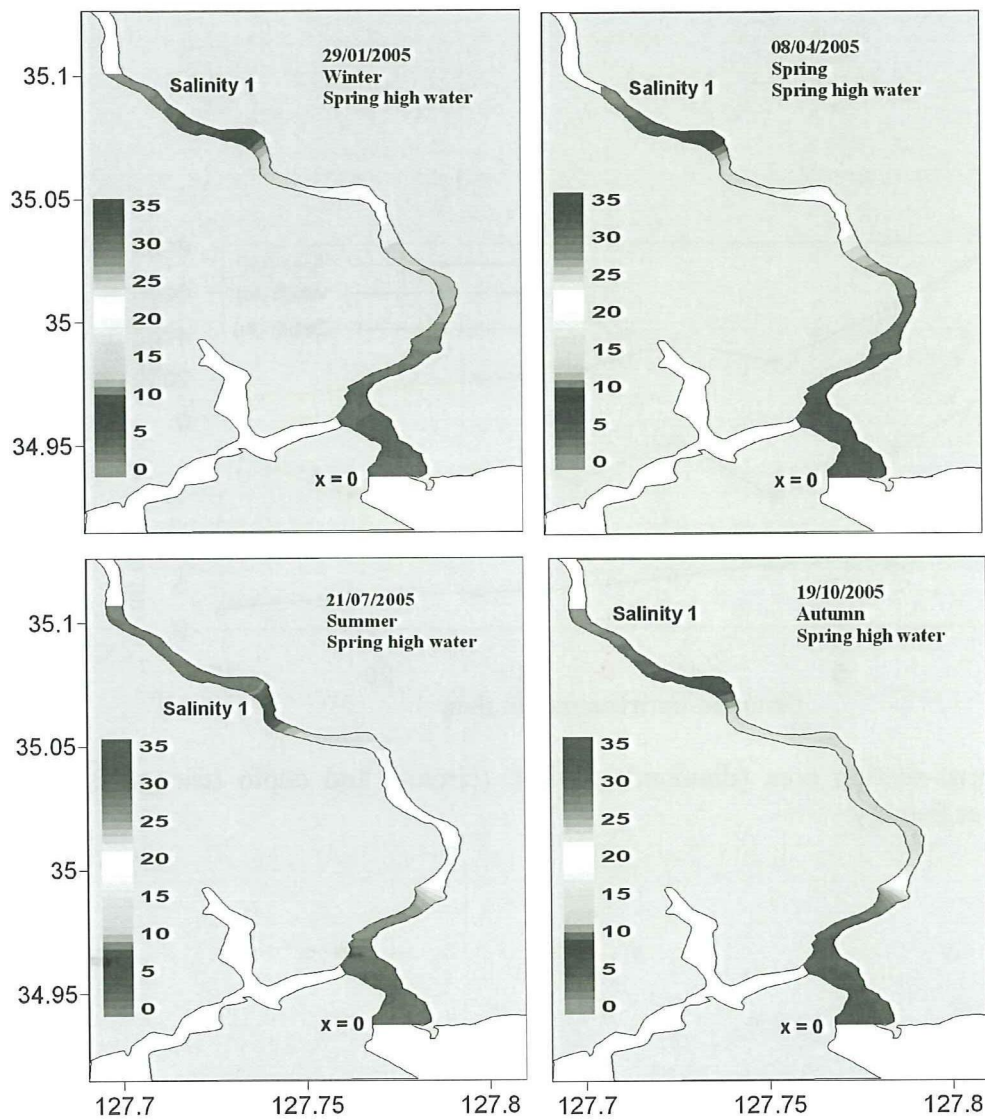
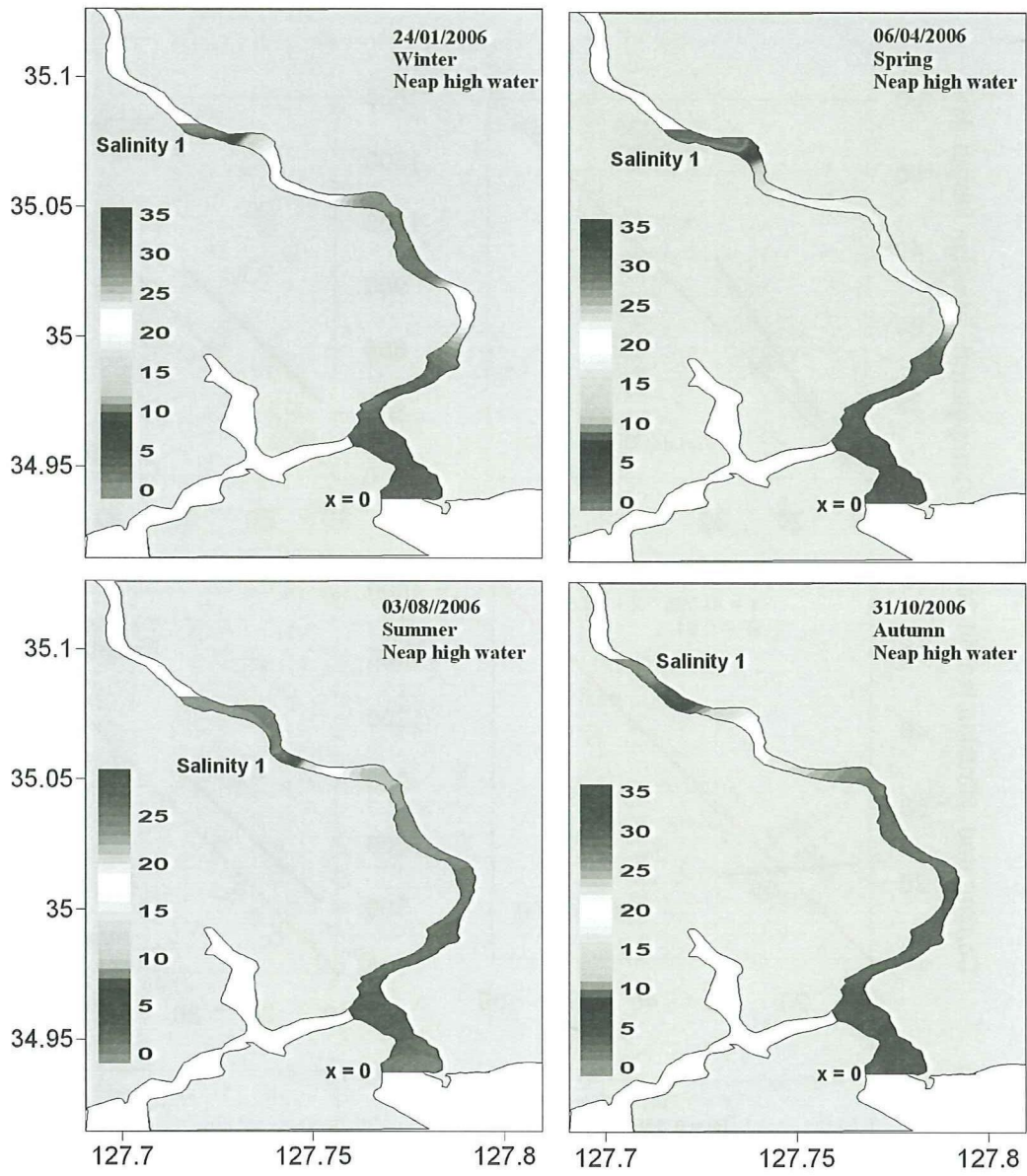


Fig. 3. Horizontal bottom salinity distribution at high water during spring tide for each season during 2005. The pink band indicates the limit of salinity 1.

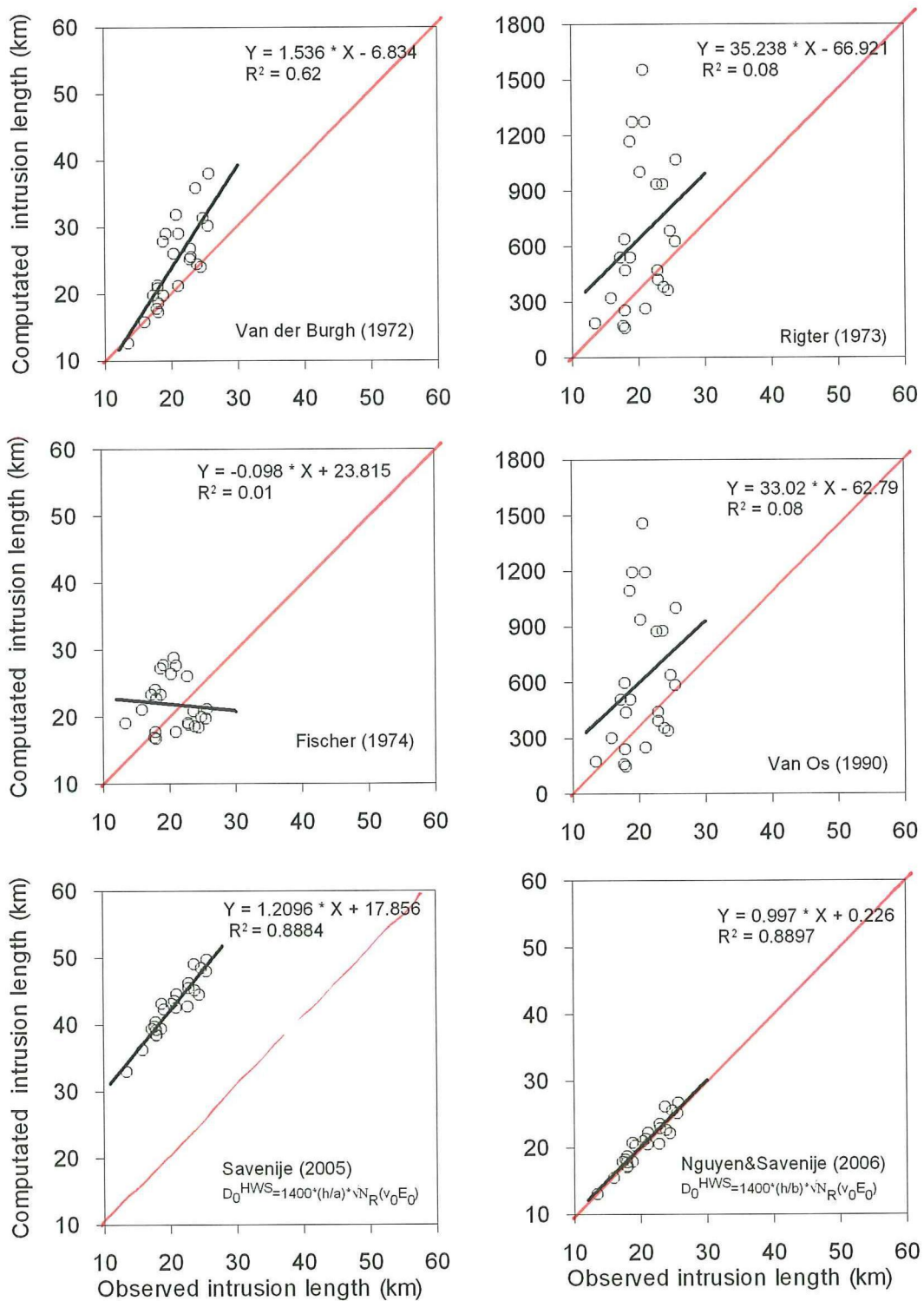
5



5 Fig. 4. Horizontal bottom salinity distribution at high water during neap tide for each season during 2006. The pink band indicates the limit of salinity 1.

10

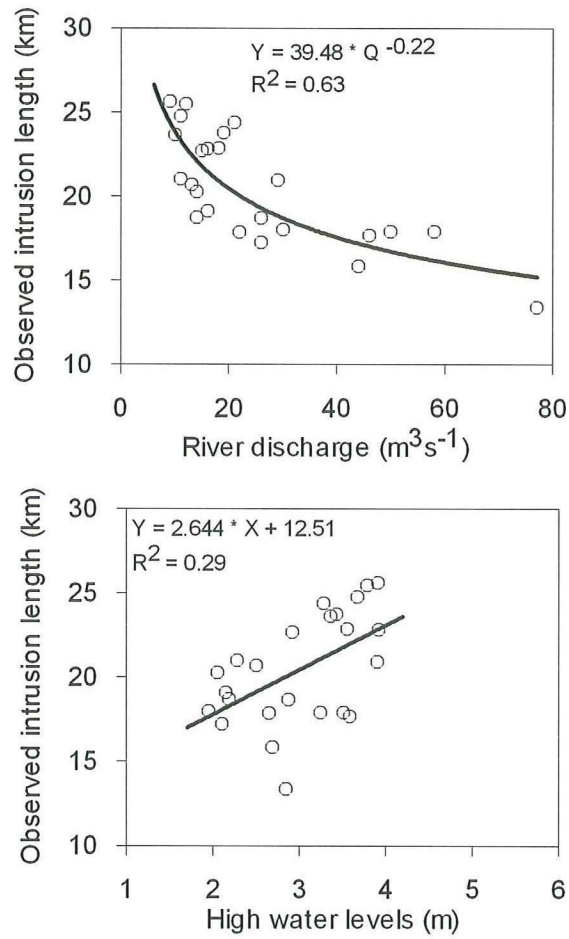
15



5 Fig. 5. Comparison of the results of various empirical models for the intrusion length measured at high water during both spring and neap tides.

lines of perfect agreement

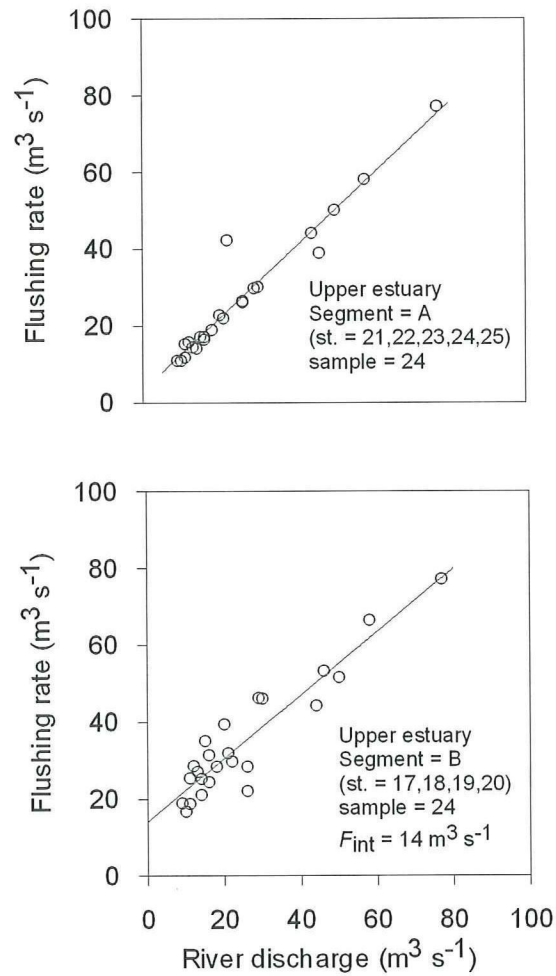
5



10 Fig. 6. The power correlation between the salt intrusion lengths measured at high water during spring-neap tides and river discharges (upper); observed salt intrusion lengths and high water levels (lower).

15

20

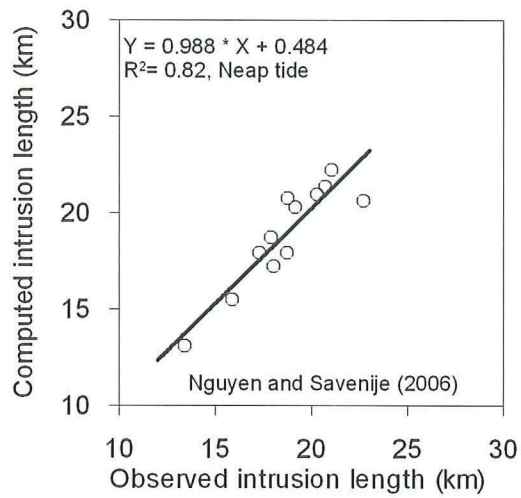
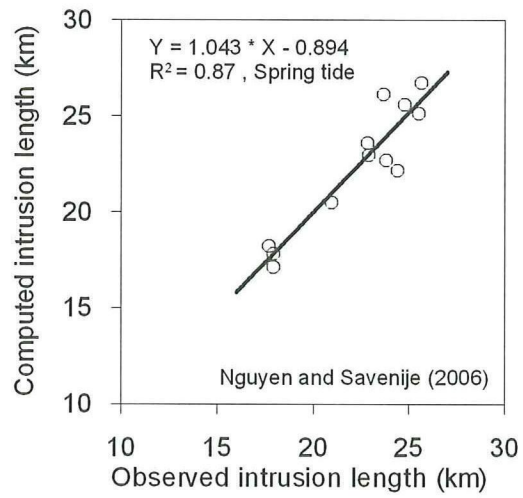


5 Fig. 7. Plot of flushing rate (F) against river discharge (R) upstream of the Sumjin River Estuary. The upper estuary, segment A, shows gravitational circulation flux where the fitting line is linear with an intercept of zero and increasing F value with increasing R value. The intercept value, F_{int} in Segment B indicates the tidal flux and the excess amount of intercept value indicates the gravitational circulation flux.

10

15

20



5 Fig. 8. Comparison of the model results with the intrusion length measured at high water during both spring and neap tides.

